Available online at www.sciencedirect.com
ScienceDirect
Trans. Nonferrous Met. Soc. China 34(2024) 1558−1570
Transactions of Nonferrous Metals Society of China
www.tnmsc.cn

Glass forming ability prediction of bulk metallic glasses based on fused strategy

Ting ZHANG, Zhi-lin LONG, Li PENG

School of Civil Engineering, Xiangtan University, Xiangtan 411105, China

Received 7 October 2022; accepted 15 March 2023

Abstract: In order to improve the prediction accuracy of random forest (RF), *k*-nearest neighbor (KNN), gradient boosted decision trees (GBDT) and extreme gradient boosting (XGBoost) models, a fused strategy was proposed for predicting the glass forming ability (GFA) of bulk metallic glasses (BMGs). Feature vectors were extracted using a trained convolutional neural network (CNN), and alloy composition information was the only variable input without requiring various physical and chemical properties acquired from experiments. Besides, the hyperparameters of RF, KNN, GBDT and XGBoost models were optimized by grid search method and *k*-fold cross validation. The obtained results show that the accuracy of CNN−RF, CNN−KNN, CNN−GBDT and CNN−XGBoost fused models proposed in this work in predicting GFA is higher than that of the four machine learning models mentioned above (i.e., RF, KNN, GBDT and XGBoost models), implying that the trained CNN could extract feature more effectively than manual feature construction. Furthermore, compared with previously reported machine learning models and GFA criteria, the proposed fused models could predict the GFA of BMG more accurately.

Key words: bulk metallic glasses; glass forming ability; machine learning; convolutional neural network; alloy composition

1 Introduction

Metallic glasses (MGs), especially bulk metallic glasses (BMGs), as a new type of structural and functional materials，have attracted extensive research enthusiasm since their discovery. Though they possess many excellent mechanical, physical and chemical properties such as extremely high strength and hardness [1], high wear and corrosion resistance [2], as well as their excellent magnetic [3] and catalytic properties [4,5], the research and development of MGs are limited due to their macroscopic brittle nature and low glass forming ability (GFA) [6,7]. Thus, how to improve the GFA of MGs and produce large-size specimens has become a hot topic.

In the past few decades, thousands of metal glass types have been developed by trial-and-error method, which is an effective and commonly used research method with extensive experiments. However, the process of trial-and-error method usually takes a long time and consumes materials. Some empirical criteria for gauging GFA have been proposed to accelerate the development cycle of MGs, such as T_{rg} (=T_g/T_l, T_g is glass transition temperature and T_l is liquidus temperature) [8], ΔT_x(=T_x-T_g, T_x is onset crystallization temperature) [9], γ(=$T_x/(T_g+T_l)$) [10], γ_m(=$(2T_x-T_g)/T_l$) [11], the enthalpy of mixing (ΔH_{mix}) [12], the enthalpy of formation of solid solution (ΔH_{ss}) [13], configurational entropy (ΔS_c) [14], mismatch entropy (S_σ) [15], atomic size difference (δ) [12], and valence electron concentration (VEC) [16]. These criteria are lack of generality and strongly rely on experimental measurements, which are not

Corresponding author: Zhi-lin LONG, Tel: +86-731-58298287, E-mail: longzl@xtu.edu.cn
DOI: 10.1016/S1003-6326(24)66491-5

easy to accurately identify. So, it is necessary to make more efforts to explore the basic properties of MGs to exploit novel MGs with high GFA.

With the development of technology and the accumulation of data, different machine learning (ML) approaches, i.e. artificial neural network [17−23], *k*-nearest neighbor (KNN) [20,24], support vector machine (SVM) [19,20,24,25], convolutional neural network (CNN) [19,21,26], decision tree (DT) [24,27], random forest (RF) [22,24,28,29], gradient boosted decision trees (GBDT) [30], extreme gradient boosting algorithm (XGBoost) [29,31,32], generative adversarial networks (GAN) [33], and reinforcement learning [34] have been extensively employed to accelerate the discovery of different materials. In particular, researchers have carried out extensive research on MGs with ML [35]. LIU et al [36] applied four ML models, namely RF, KNN, GBDT and XGBoost to predict GFA of amorphous alloys, respectively. LI et al [37] used XGBoost, artificial neural networks (ANN) and RF to predict the magnetic properties of Fe-based MGs with consideration of GFA. While the effectiveness of the general ML model in materials science has been confirmed, and the multilayer network model with more complex structure has also been used for research. LIU et al [38] trained a back propagation neural network model (BPNN) based on a dataset assembled from thousands of ternary alloys and accurately identified the MG and non-MG classes. SAMAVATIAN et al [39] proposed a new correlation-based neural network (CBNN) approach to assess critical casting thickness (D_{max}), reduced glass transition temperature, and elastic modulus. These studies show that ML approaches have great potential in searching for new MGs and evaluating their properties.

In this work, a fused strategy combining CNN model and traditional ML model is proposed. The alloy composition information is used as the only variable input, which takes into account the possible combination space of 100 alloy elements from element H to element Fm. Then, the trained CNN model is used to extract feature vectors, and the above feature vectors are used as the input of traditional ML model to predict D_{max} of amorphous alloy, which avoids manual feature extraction. RF, KNN, GBDT and XGBoost are four traditional ML models mainly considered in this work, and they are optimized by grid search method and *k*-fold cross validation (k=10). In addition, the impact of different features obtained from different hidden layers of CNN on the results is explored. Finally, by comparing the fused models with the four above-mentioned ML models and some previous reported models/criteria, the potential significance of our framework in developing large MGs with GFA is highlighted.

2 Dataset and ML framework

2.1 Dataset

The glass formation dataset used in this work is based on the dataset of ZHANG et al [40]. 1888 amorphous alloy samples with D_{max} value greater than 1 mm include 622 Fe-, 279 Zr-, 184 Cu-, 142 Mg-, 142 Ti-, 95 La-, 80 Ni-, 67 Ca-, 58 Ce-, 56 Co-, 28 Gd-, 20 Pd-, 15 Nd-, 13 Mn-, 12 Pr-, 11 Tb-, 7 Au-, 6 Hf-, 6 CoFe-, 5 Y-, 5 Yb-, 5 Er-, 4 Ag-, 4 Ho-, 4 Sm-, 4 Pt-, 4 Cr-, 3 Dy-, 2 Tm-, 2 Sc-, 1 Mo-, 1 Be-, and 1 Zn-based alloys. Figure 1 shows the distribution of D_{max}. It can be found that the samples with D_{max} between 1 and 5 mm account for the vast majority, reaching 72.19%, the samples with D_{max} between 5 and 20 mm account for 25.85%, and the samples with D_{max} more than 20 mm only account for 1.96%. Obviously, the data distribution is unbalanced with a positive skewness value of 5.193. There may be intensive training for the amorphous alloy samples with smaller D_{max}, while insufficient training for samples with larger D_{max}, resulting in overfitting or underfitting [41].

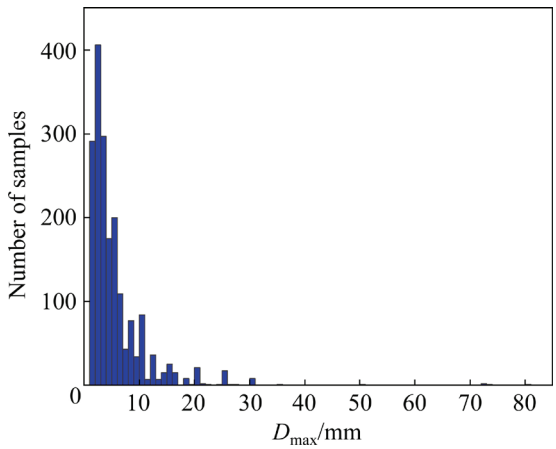

Fig. 1 D_{max} distribution in dataset

2.2 ML framework

Due to their characteristics of simple structure, easy implementation and low computational cost,

traditional machine learning models such as RF and KNN have shown strong performance in different tasks and great potential in promoting the development of materials science. Generally, the key and appropriate feature descriptors, which are media that link material composition with material properties, are extracted from the influencing factors created based on domain knowledge, and used as the input of ML to derive the relationship between the feature descriptors and the target attributes. For instance, the physical and chemical factors, such as atomic size difference and melting temperature are selected to predict the GFA in the field of MGs. Thus, when the traditional ML model is applied, the basic qualities of the corresponding background common sense and theoretical knowledge are strictly required for researchers to select more appropriate feature descriptors.

The recently developed CNN is likely useful to directly learn the most useful spatial statistics objectively from the available data [42]. CNN is an end-to-end learning model, which produces a more advanced feature extraction method and can extract more complex features from the input space. The parameters of feature extraction are obtained through training data learning, which avoids manual feature extraction. CNN model has also been proved to provide guidance for the development and preparation of amorphous alloys in previous studies [19,21,26,40]. Despite a costly initial training cycle, deployment and utilization of learned CNN models are very efficient, and the filters learned by CNNs can be used as permanent feature embedding with a sufficiently large dataset [42]. Therefore, we consider combining CNN as a feature extractor with traditional ML to predict GFA more accurately.

Figure 2 illustrates the workflow of the proposed the fused ML framework. The first step is to preprocess the dataset. The percentage of amorphous alloy elements from element H to element Fm is taken into account and mapped to a 10×10 feature graph, which can search for possible amorphous alloys in a wide range of spaces. Secondly, a trained CNN model is used to extract feature vectors from the above feature map. Therefore, the trained CNN model is required to accurately describe the relationship between the dataset and the feature vectors. Finally, the corresponding feature vectors are used as the input of the traditional ML model for the fitting of $D_{\max}$. The same procedure is used for prediction.

The ML approach is implemented by using the Scikit-learn ML framework. In order to avoid repeated work, the trained CNN model obtained in previous work [40] is directly adopted. Since the ability of the trained CNN model to accurately predict the GFA of BMGs has been verified in previous work, the feature vectors extracted from the hidden layer of the model certainly have the representation ability for GFA. Besides, taking the percentage of amorphous alloy elements as the only input variable can reduce the demand for some physical parameters obtained in experiment. RF, KNN, GBDT and XGBoost are the four traditional ML algorithms selected in this work, and their hyperparameters will be optimized by grid search method and *k*-fold cross validation (k=10). Generally, the process of grid search is time-consuming. In order to reduce the calculation cost, we optimize the hyperparameter values in a small range based on the hyperparameter values in Ref. [36]. Moreover, 10-fold cross validation is employed to evaluate the performance of ML models in the work. As shown in Fig. 3, the dataset is divided into 10 parts without repetition. In the *k*th iteration, the *k*th part of dataset is used as the test set, and the remaining data is used as the training set. The final evaluation is given on average according to the estimation of 10 rounds.

2.3 Model evaluation index

Three regression evaluation indexes are used to evaluate the performance of model and expressed as follows:

$$E_{\mathrm{MAE}}=\frac{1}{n}\sum_{i=1}^{n}\left|\hat{y}_i-y_i\right| \tag{1}$$

$$E_{\mathrm{RMSE}}=\sqrt{\sum_{i=1}^{n}\frac{1}{n}\left(\hat{y}_i-y_i\right)^2} \tag{2}$$

$$R^2=1-\sum_{i=0}^{n-1}(y_i-\hat{y}_i)^2\Big/\sum_{j=0}^{n-1}(y_i-\overline{y})^2 \tag{3}$$

where E_{MAE} is the mean absolute error, E_{RMSE} is the root mean absolute error, R^2 is the coefficient of determination, n is the number of samples, $\hat{y}_i$ is the ith predicted value, y_i is the ith measured value, and $\overline{y}$ is the average value of all measured values.

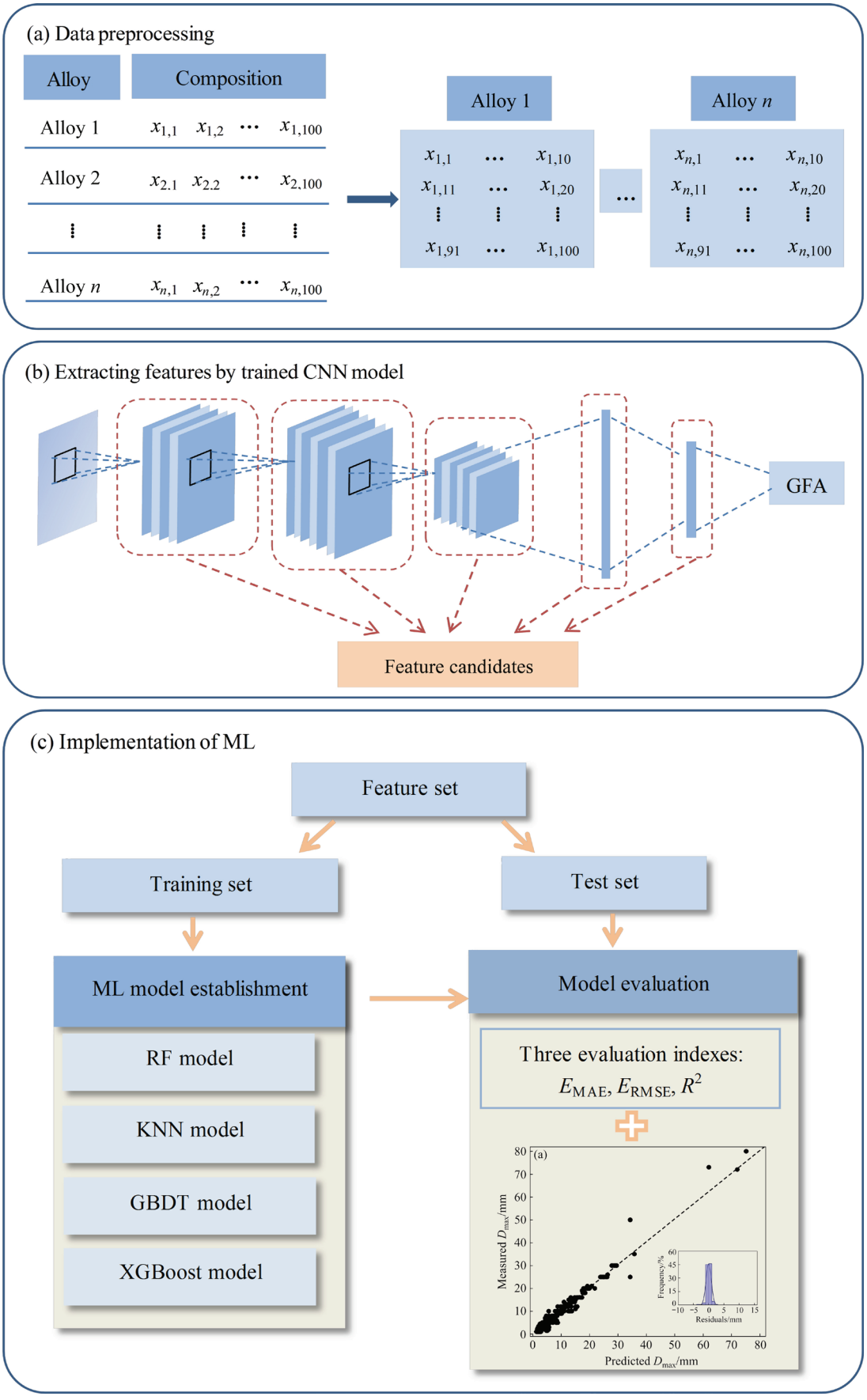

Fig. 2 Workflow of proposed fused ML framework

While the closer to 0 the values of E_{MAE} and E_{RMSE} are, the smaller the error is, and the closer to 1 the value of R^2 is, the better the model is.

3 Results and discussion

3.1 D_{max} prediction of fused models

The whole BMGs dataset is randomly divided into training set and test set with a ratio of 8:2, where the training set is used for model training and the test set is used for the predictive performance of the model. The training set and test set are disjoint, which ensures that the test set can objectively evaluate the prediction performance of each trained model. The optimal hyperparameter combination of ML model is determined by training the model on the training set through grid search method and 10-fold cross validation. As we all know, some hyperparameters for algorithms have more influence on the results, while some have less influence. In order to reduce the computational cost, only a part of hyperparameters for algorithms are optimized based on literature [36]. Through grid search method and 10-fold cross validation, the hyperparameter combinations of RF, KNN, GBDT and XGBoost with the highest scores are shown in Table 1.

Figure 4 shows the CNN model structure obtained in previous work [40] and the change process of its data. The hidden layers, except for the input layer and the output layer, are labeled as h1, h2, h3, h4 and h5, respectively. And in our code, the features of different hidden layers with the

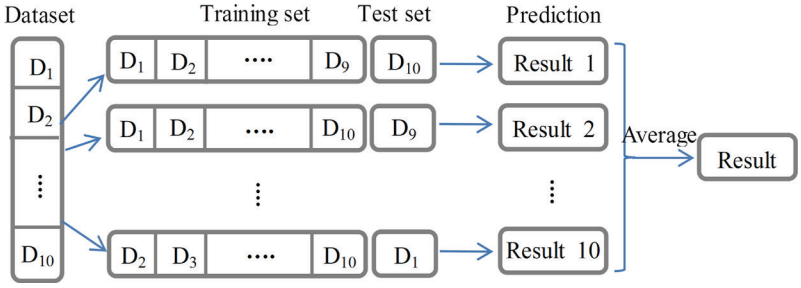

Fig. 3 Workflow of 10-fold cross validation

Table 1 Optimal hyperparameters through grid search method for RF, KNN, GBDT and XGBoost models

Model	Hyperparameter			
RF	*n*_estimators = 54	max_depth = 15		
KNN	*n*_estimators = 12	weights = 'distance'		
GBDT	*n*_estimators = 55	learning_rate = 0.11	loss = 'lad'	max_depth = 25
XGBoost	*n*_estimators = 18	max_depth = 8	learning_rate = 0.1	reg_lambda = 0.32

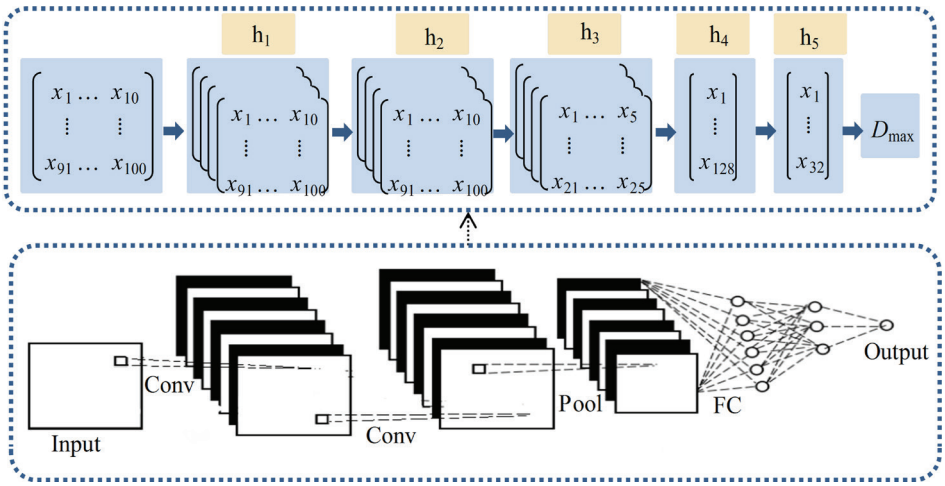

Fig. 4 Structure of CNN model obtained in previous work [40] and change process of its data

10×10 feature graphs constructed by the element percentage as the input of CNN model are obtained by the model.get_layer() function of the Python deep learning API named Keras. Then, these features are converted into vectors and used as the input of RF, KNN, GBDT and XGBoost models to explore the impact of features with different layers on the model.

The training and test R^2 values of the feature vectors with different hidden layers for different models are shown in Fig. 5. It was found that the R^2 value of the h3 layer decreased slightly and then gradually increased to the maximum value at the h5 layer. We suggest that although the calculation efficiency is improved through the pooling operation of the h3 layer, the direct reduction of the dimension also has a certain impact on the results. Then, the full connection layers integrate the information, resulting in the improvement of the R^2 of the next few layers. In addition, the model is trained as a whole, so it is obvious that the feature vectors of the last hidden layer h5 are the most representative and serve as the final input of the general machine learning models.

The final fused models are called CNN−RF, CNN−KNN, CNN−GBDT and CNN−XGBoost models and the results of them are shown in Figs. 6−9 and Table 2 in detail. In these figures, the x-axis represents the predicted values of D_{max} by the above models and the y-axis represents the measured values of D_{max}. An auxiliary dotted line is also added with the equation $y=x$. The closer the point to the dotted line is, the better the prediction is. Besides, the distributions of the residuals (Residuals are computed as the difference between measured D_{max} and predicted D_{max}) are depicted in the corresponding subplots. The results show that these fused models have good fitting effects with the training R^2 values greater than 0.9 and the test R^2 values greater than 0.85.

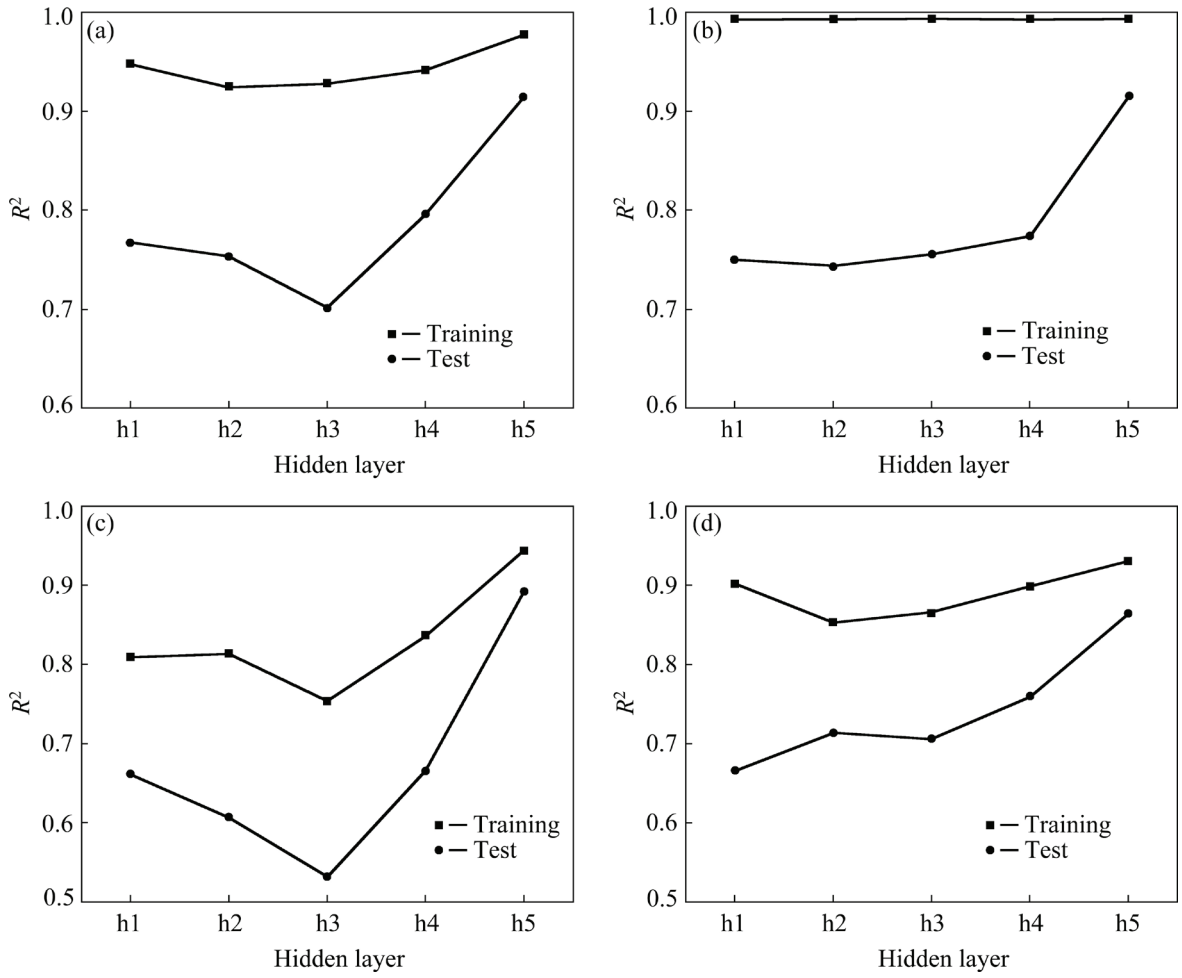

Fig. 5 Training and test R^2 values of feature vectors with different hidden layers for RF (a), KNN (b), GBDT (c) and XGBoost (d) models

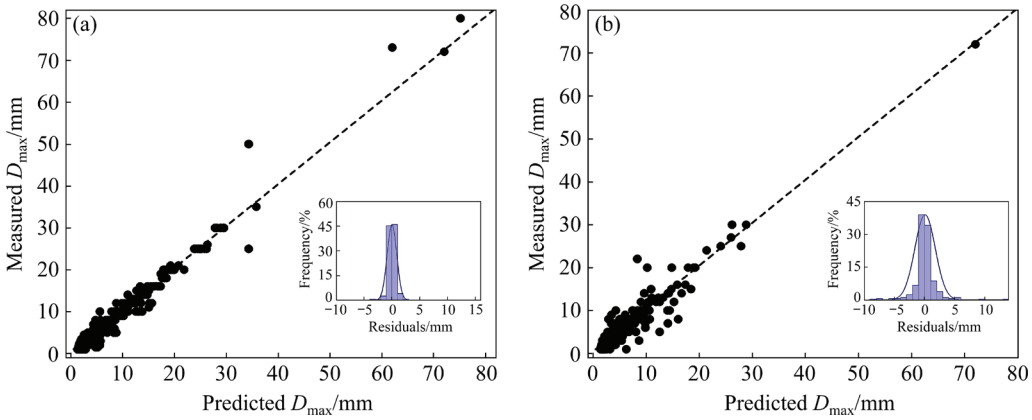

Fig. 6 Comparison between measured and predicted values by CNN−RF model based on training set (a) and test set (b)

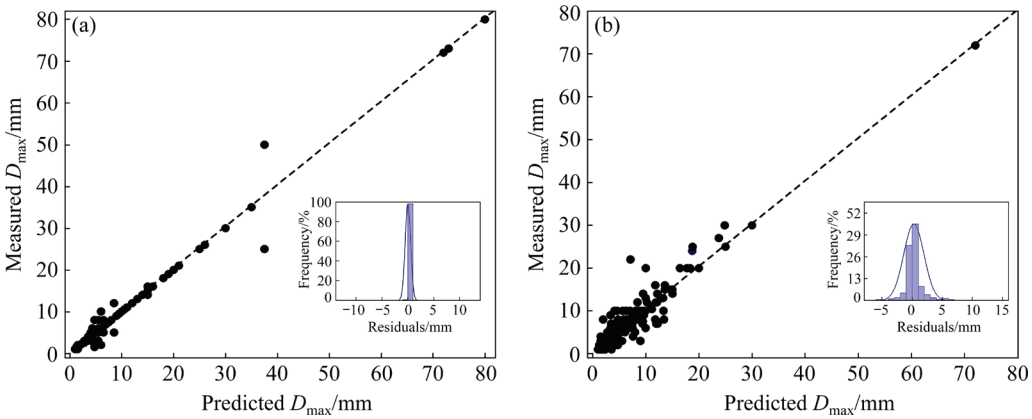

Fig. 7 Comparison between measured and predicted values by CNN−KNN model based on training set (a) and test set (b)

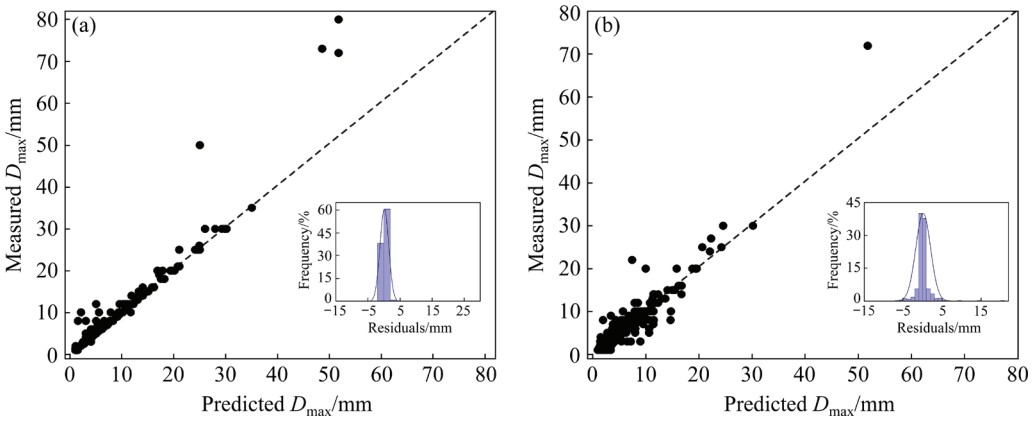

Fig. 8 Comparison between measured and predicted values by CNN−GBDT model based on training set (a) and test set (b)

3.2 Performance comparison of fused models for predicting GFA of BMGs

In order to illustrate the advantages of the proposed model framework, the traditional RF, KNN, GBDT and XGBoost models are used for prediction under the same conditions, and the corresponding results are shown in Figs. 10−13 and Table 3. The results show that these traditional models also predict well, with the training R^2 values greater than 0.8 and the test R^2 values greater than 0.7. However, the corresponding comparison between the tables of the two groups of models displays that the training and test R^2 values of the fused models increased by 15.67%, 17.12%, 12.95% and 14.26%, respectively, compared with the traditional ML models. It can also be seen intuitively from the figures that compared with the traditional ML models, the data points of the fused

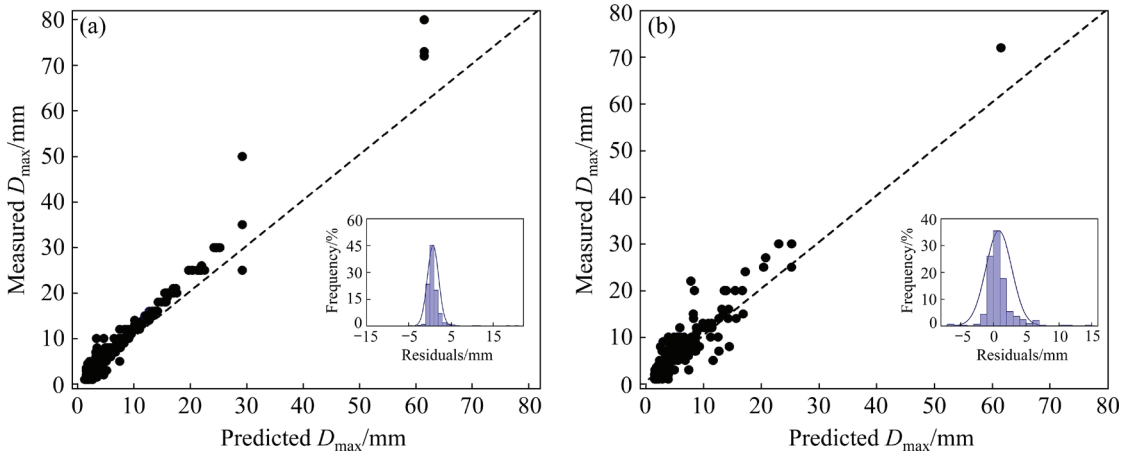

Fig. 9 Comparison between measured and predicted values by CNN−XGBoost model based on training set (a) and test set (b)

Table 2 Values of E_{MAE}, E_{RMSE} and R^2 obtained for CNN−RF, CNN−KNN, CNN−GBDT and CNN−XGBoost models

Model	Training set			Test set		
	E_{MAE}/mm	E_{RMSE}/mm	R^2	E_{MAE}/mm	E_{RMSE}/mm	R^2
CNN−RF	0.4319	0.7455	0.9775	0.9596	1.6948	0.9144
CNN−KNN	0.0471	0.2826	0.9915	0.9047	1.6965	0.9142
CNN−GBDT	0.1787	1.8746	0.9435	0.8889	1.9049	0.8918
CNN−XGBoost	0.9445	2.3031	0.9305	1.2972	2.1354	0.8641

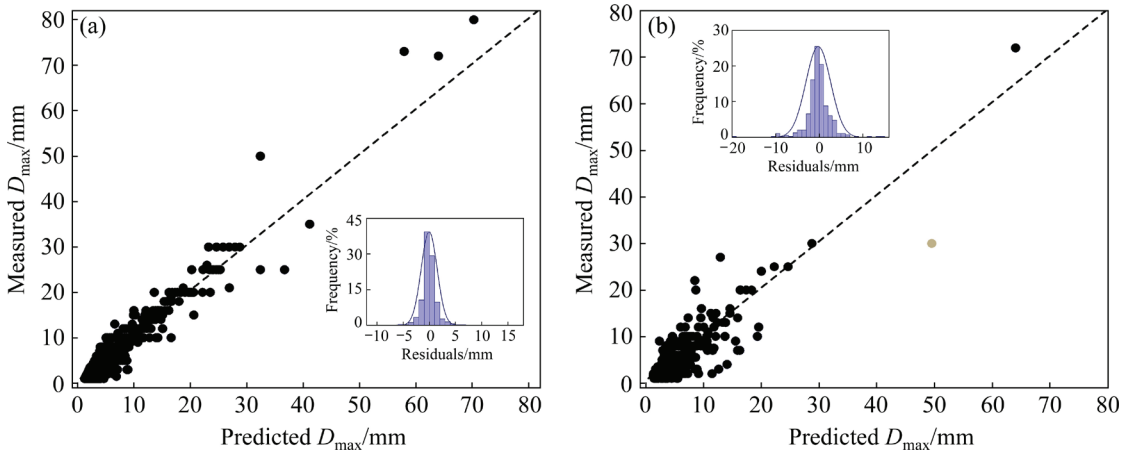

Fig. 10 Comparison between measured and predicted values by RF model based on training set (a) and test set (b)

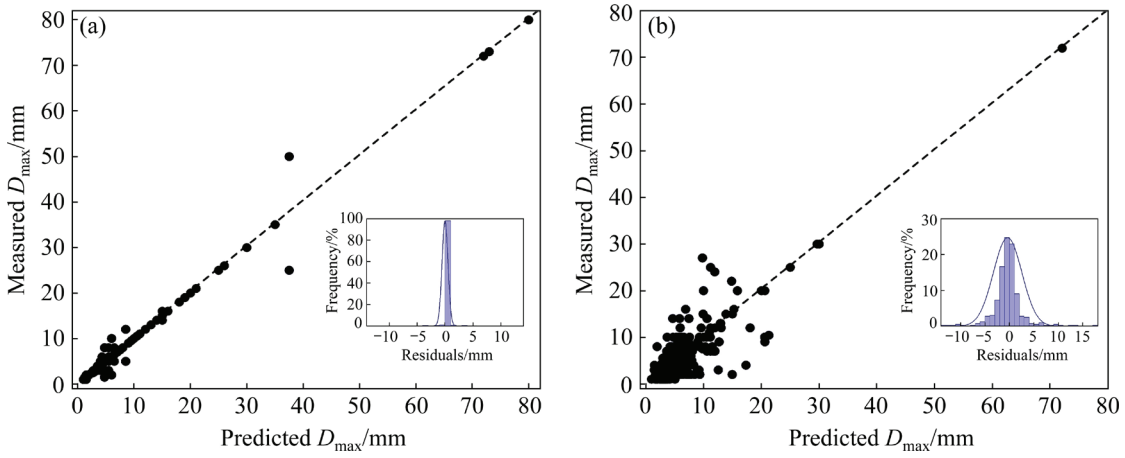

Fig. 11 Comparison between measured and predicted values by KNN model based on training set (a) and test set (b)s

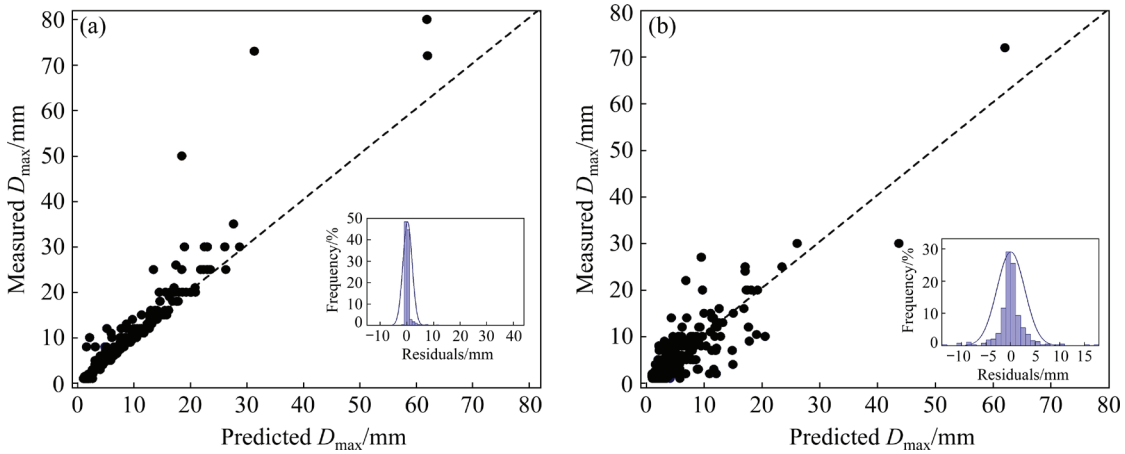

Fig. 12 Comparison between measured and predicted values by GBDT model based on training set (a) and test set (b)

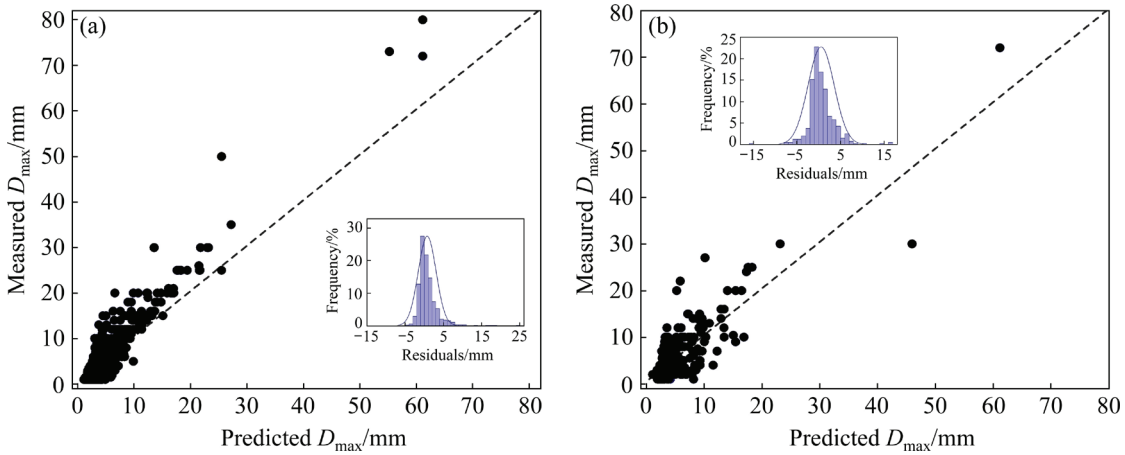

Fig. 13 Comparison between measured and predicted values by XGBoost model based on training set (a) and test set (b)

Table 3 Values of E_{MAE}, E_{RMSE} and R^2 obtained for traditional ML models of RF, KNN, GBDT and XGBoost

Model	Training set			Test set		
	E_{MAE}/mm	E_{RMSE}/mm	R^2	E_{MAE}/mm	E_{RMSE}/mm	R^2
RF	0.9570	2.3289	0.9298	1.8057	2.8511	0.7577
KNN	0.0471	0.2826	0.9915	1.78087	2.9361	0.7430
GBDT	0.3604	3.0467	0.9081	1.6452	2.8239	0.7623
XGBoost	1.5537	5.9877	0.8194	2.0271	3.0566	0.7215

models are more concentrated and closer to the straight dotted line $y=x$ in both the training set and the test set. This proves that CNN has the function of feature learning and extraction, and can improve the fitting effect when combined with the traditional ML model.

Furthermore, we can also compare the fused models with other GFA criteria or ML methods in the previous literature [43−46]. LONG et al [43], DENG et al [44], MASTROPIETRO and MOYA [45], and MAJID et al [46] have reported their R^2 values of 0.42759, 0.43244, 0.90000, and 0.57790 respectively on their entire datasets, as shown in Table 4. We obtained four different datasets from Refs. [43−46] and used them as inputs of the fused models in this work, respectively. The results are shown in Fig. 14, which shows that the R^2 values of the fused models based on four

Table 4 Relevant information of previous literature

Number of BMGs	Criterion	R^2	Ref.
622	χ	0.42759	[43]
665	ω	0.43244	[44]
480	Ensemble model	0.90000	[45]
349	GRNN	0.57790	[46]

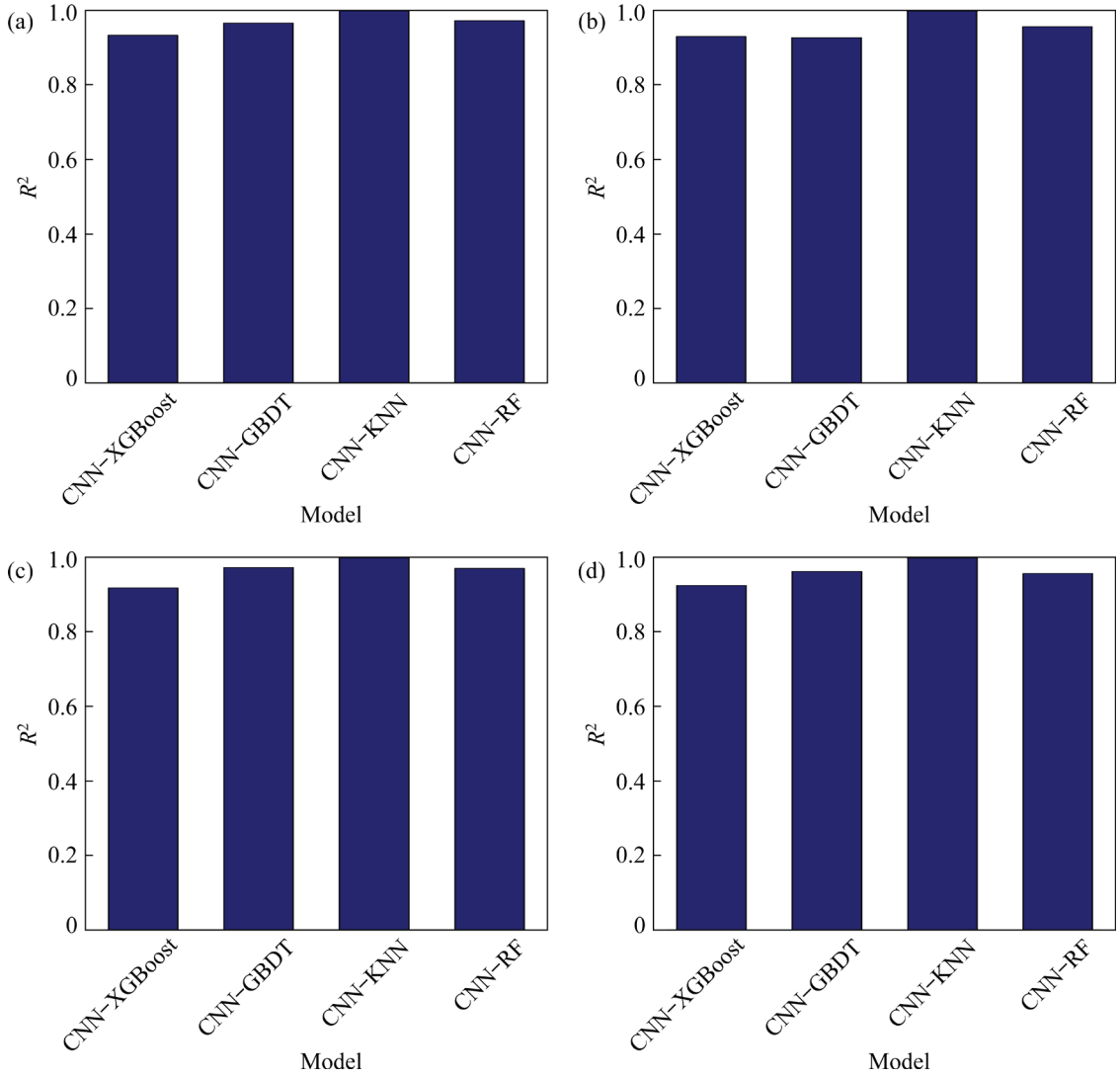

Fig. 14 Values of R^2 obtained by fused models based on datasets in Ref. [43] (a), Ref. [44] (b), Ref. [45] (c) and Ref. [46] (d)

datasets are greater than 0.9 and are higher than the R^2 values in the original literature. This proves that our strategy has greater potential in predicting GFA of BMG than other GFA criteria or ML methods.

4 Conclusions

(1) Four fused models, namely CNN−RF, CNN−KNN, CNN−GBDT and CNN−XGBoost were proposed and trained to predict the GFA of BMGs. The results show that these models possess excellent prediction performance, with the training R^2 values greater than 0.9 and the test R^2 values greater than 0.85.

(2) Alloy composition is the only variable input. Therefore, the suggested framework can be applicable to different BMGs as long as the constituent elements in these BMGs lie in element range from H to Fm in the periodic table.

(3) The trained CNN models are very efficient, and the corresponding filters can be used as feature embedding of RF, KNN, GBDT and XGBoost models, avoiding manual feature extraction. In the meantime, the features extracted from the last hidden layer of the learned CNNs are more representative than those of other hidden layers.

(4) Compared with RF, KNN, GBDT and XGBoost models, the prediction accuracy of CNN−RF, CNN−KNN, CNN−GBDT and CNN−XGBoost models increased by 15.67%, 17.12%, 12.95% and 14.26%, respectively. Compared with the previous reported models and/or criteria, the four proposed fused models also have better performance in predicting the GFA of BMG.

CRediT authorship contribution statement

Ting ZHANG: Conceptualization, Investigation, Methodology, Data curation, Visualization, Writing − Original draft; **Zhi-lin LONG:** Conceptualization, Writing − Review & editing, Supervision; **Li PENG:** Data curation.

Declaration of competing interest

The authors declare that they have no known competing financial interests or personal relationships that could have appeared to influence the work reported in this paper.

Acknowledgments

This research was supported by the National Natural Science Foundation of China (No. 51971188), and the Postgraduate Scientific Research Innovation Project of Hunan Province, China (No. CX20200649). All these supports are acknowledged.

References

[1] DUN Chao-chao, LIU Hai-shun, HOU Long, XUE Lin, DOU Lin-tao, YANG Wei-ming, ZHAO Yu-cheng, SHEN Bao-long. Ductile Co−Nb−B bulk metallic glass with ultrahigh strength [J]. Journal of Non-Crystalline Solids, 2014, 386: 121−123.

[2] KHAN M M, NEMATI A, RAHMAN Z U, SHAH U H, ASGAR H, HAIDER W. Recent advancements in bulk metallic glasses and their applications: A review [J]. Critical Reviews in Solid State and Materials Sciences, 2018, 43(3): 233−268.

[3] LI H X, LU Z C, WANG S L, WU Y, LU Z P. Fe-based bulk metallic glasses: Glass formation, fabrication, properties and applications [J]. Progress in Materials Science, 2019, 103: 235−318.

[4] YANG Wei-ming, WANG Qian-qian, LI Wen-yu, XUE Lin, LIU Hai-shun, ZHOU Jing, MO Jin-yong, SHEN Bao-long. A novel thermal-tuning Fe-based amorphous alloy for automatically recycled methylene blue degradation [J]. Materials & Design, 2019, 161: 136−146.

[5] JIA Zhe, DUAN Xiao-guang, QIN Peng, ZHANG Wen-chang, WANG Wei-min, YANG Chao, SUN Hong-qi, WANG Shao-bin, ZHANG Lai-Chang. Disordered atomic packing structure of metallic glass: Toward ultrafast hydroxyl radicals production rate and strong electron transfer ability in catalytic performance [J]. Advanced Functional Materials, 2017, 27(38): 1702258.

[6] HUANG Yong-jiang, NING Zhi-liang, SHEN Zhe, LIANG Wei-zhong, SUN Hai-cao, SUN Jian-fei. Bending behavior of as-cast and annealed ZrCuNiAl bulk metallic glass [J]. Journal of Materials Science & Technology, 2017, 33(10): 1153−1158.

[7] SUN B A, WANG W H. The fracture of bulk metallic glasses [J]. Progress in Materials Science, 2015, 74: 211−307.

[8] TURNBULL D. Under what conditions can a glass be formed? [J]. Contemporary Physics, 1969, 10(5): 473−488.

[9] INOUE A, ZHANG T, MASUMOTO T. Glass-forming ability of alloys [J]. Journal of Non-Crystalline Solids, 1993, 156: 473−480.

[10] LU Z P, LIU C T. A new glass-forming ability criterion for bulk metallic glasses [J]. Acta Materialia, 2002, 50(13): 3501−3512.

[11] DU X H, HUANG J C, LIU C T, LU Z P. New criterion of glass forming ability for bulk metallic glasses [J]. Journal of Applied Physics, 2007, 101: 086108.

[12] INOUE A. Stabilization of metallic supercooled liquid and bulk amorphous alloys [J]. Acta Materialia, 2000, 48(1): 279−306.

[13] MIEDEMA A R, de BOER F R, BOOM R. Model predictions for the enthalpy of formation of transition metal alloys [J]. Calphad, 1977, 1(4): 341−359.

[14] RAMAKRISHNA RAO B, GANDHI A S, VINCENT S, BHATT J, MURTY B S. Prediction of glass forming ability using thermodynamic parameters [J]. Transactions of the Indian Institute of Metals, 2012, 65(6): 559−563.

[15] MANSOORI G A, CARNAHAN N F, STARLING K E, LELAND T W Jr. Equilibrium thermodynamic properties of the mixture of hard spheres [J]. The Journal of Chemical Physics, 1971, 54(4): 1523−1525.

[16] GUO S, LIU C T. Phase stability in high entropy alloys: Formation of solid-solution phase or amorphous phase [J]. Progress in Natural Science: Materials International, 2011, 21(6): 433−446.

[17] ISLAM N, HUANG W J, ZHUANG H L. Machine learning for phase selection in multi-principal element alloys [J]. Computational Materials Science, 2018, 150: 230−235.

[18] CASSAR D R, de CARVALHO A C, ZANOTTO E D. Predicting glass transition temperatures using neural networks [J]. Acta Materialia, 2018, 159: 249−256.

[19] ZHOU Zi-qing, ZHOU Ye-ju, HE Quang-feng, DING Zhao-yi, LI Fu-cheng, YANG Yong. Machine learning guided appraisal and exploration of phase design for high entropy alloys [J]. NPJ Computational Materials, 2019, 5: 128.

[20] HUANG W J, MARTIN P, ZHUANG H L. Machine-learning phase prediction of high-entropy alloys [J]. Acta Materialia, 2019, 169: 225−236.

[21] LU Fei, LIANG Yong-chao, WANG Xing-ying, GAO Ting-hong, CHEN Qian, LIU Yun-chun, ZHOU Yu, YUAN Yong-kai, LIU Yu-tao. Prediction of amorphous forming ability based on artificial neural network and convolutional neural network [J]. Computational Materials Science, 2022, 210: 111464.

[22] AYDIN F, DURGUT R. Estimation of wear performance of AZ91 alloy under dry sliding conditions using machine learning methods [J]. Transactions of Nonferrous Metals Society of China, 2021, 31(1): 125−137.

[23] QUAN Guo-zheng, ZHANG Pu, MA Yao-yao, ZHANG Yu-qing, LU Chao-long, WANG Wei-yong. Characterization of grain growth behaviors by BP-ANN and Sellars models

for nickel-base superalloy and their comparisons [J]. Transactions of Nonferrous Metals Society of China, 2020, 30(9): 2435−2448.

[24] MACHAKA R. Machine learning-based prediction of phases in high-entropy alloys [J]. Computational Materials Science, 2021, 188: 110244.

[25] JAHED ARMAGHANI D, ASTERIS P G, ASKARIAN B, HASANIPANAH M, TARINEJAD R, HUYNH V V. Examining hybrid and single SVM models with different kernels to predict rock brittleness [J]. Sustainability, 2020, 12(6): 2229.

[26] ZENG Shu-ming, ZHAO Yin-chang, LI Geng, WANG Rui-rui, WANG Xin-ming, NI Jun. Atom table convolutional neural networks for an accurate prediction of compounds properties [J]. NPJ Computational Materials, 2019, 5: 84.

[27] WARD L, AGRAWAL A, CHOUDHARY A, WOLVERTON C. A general-purpose machine learning framework for predicting properties of inorganic materials [J]. NPJ Computational Materials, 2016, 2: 1−7.

[28] LI Zhuang, LONG Zhi-lin, LEI Shan, ZHANG Ting, LIU Xiao-wei, KUANG Du-min. Predicting the glass formation of metallic glasses using machine learning approaches [J]. Computational Materials Science, 2021, 197: 110656.

[29] LI Xin, SHAN Guang-cun, ZHAO Hong-bin, SHEK C H. Domain knowledge aided machine learning method for properties prediction of soft magnetic metallic glasses [J]. Transactions of Nonferrous Metals Society of China, 2023, 33(1): 209−219.

[30] LIU X W, LONG Z L, ZHANG W, YANG L M. Key feature space for predicting the glass-forming ability of amorphous alloys revealed by gradient boosted decision trees model [J]. Journal of Alloys and Compounds, 2022, 901: 163606.

[31] LU Zhi-chao, CHEN Xin, LIU Xiong-jun, LIN De-ye, WU Yuan, ZHANG Yi-bo, WANG Hui, JIANG Sui-he, LI Hong-xiang, WANG Xian-zhen, LU Zhao-ping. Interpretable machine-learning strategy for soft-magnetic property and thermal stability in Fe-based metallic glasses [J]. NPJ Computational Materials, 2020, 6(1): 187.

[32] XIONG Jie, SHI San-qiang, ZHANG Tong-yi. Machine learning prediction of glass-forming ability in bulk metallic glasses [J]. Computational Materials Science, 2021, 192: 110362.

[33] PRYKHODKO O, JOHANSSON S V, KOTSIAS P C, ARÚS-POUS J, BJERRUM E J, CHEN H M. A denovo molecular generation method using latent vector based generative adversarial network [J]. Journal of Cheminformatics, 2019, 11(1): 1−13.

[34] ZHANG Peng, ZHANG Rui. Feature selection based on reinforcement learning and its application in material informatics [J]. Journal of Shanghai University (Natural Science Edition), 2022, 28(3): 463−475. (in Chinese)

[35] WU Jia-qi, WANG Wei-hua, SUN Yi-tao, LI Mao-zhi. Application of machine learning approach in disordered materials [J]. Scientia Sinica Physica, Mechanica & Astronomica, 2020, 50: 067002.

[36] LIU Xiao-wei, LONG Zhi-lin, YANG Ling-ming, ZHANG Wei, LI Zhuang. Prediction of glass forming ability in amorphous alloys based on different machine learning algorithms [J]. Journal of Non-Crystalline Solids, 2021, 570: 121000.

[37] LI Xin, SHAN Guang-cun, SHEK C H. Machine learning prediction of magnetic properties of Fe-based metallic glasses considering glass forming ability [J]. Journal of Materials Science & Technology, 2022, 103: 113−120.

[38] LIU Xiao-di, LI Xin, HE Quang-feng, LIANG Dan-dan, ZHOU Zi-qing, MA Jiang, YANG Yong, SHEN Jun. Machine learning-based glass formation prediction in multicomponent alloys [J]. Acta Materialia, 2020, 201: 182−190.

[39] SAMAVATIAN M, GHOLAMIPOUR R, SAMAVATIAN V. Discovery of novel quaternary bulk metallic glasses using a developed correlation-based neural network approach [J]. Computational Materials Science, 2021, 186: 110025.

[40] ZHANG Ting, LONG Zhi-lin, PENG Li, LI Zhuang. Prediction of glass forming ability of bulk metallic glasses based on convolutional neural network [J]. Journal of Non-Crystalline Solids, 2022, 595: 121846.

[41] DENG Bing-hui, ZHANG Ya-li. Critical feature space for predicting the glass forming ability of metallic alloys revealed by machine learning [J]. Chemical Physics, 2020, 538: 110898.

[42] CECEN A, DAI H J, YABANSU Y C, KALIDINDI S R, SONG L. Material structure-property linkages using three-dimensional convolutional neural networks [J]. Acta Materialia, 2018, 146: 76−84.

[43] LONG Zhi-lin, LIU Wei, ZHONG Ming, ZHANG Yun, ZHAO Ming-sheng-zi, LIAO Guang-kai, CHEN Zhuo. A new correlation between the characteristics temperature and glass-forming ability for bulk metallic glasses [J]. Journal of Thermal Analysis and Calorimetry, 2018, 132(3): 1645−1660.

[44] DENG Rui-jie, LONG Zhi-lin, PENG Li, KUANG Du-min, REN Bai-yu. A new mathematical expression for the relation between characteristic temperature and glass-forming ability of metallic glasses [J]. Journal of Non-Crystalline Solids, 2020, 533: 119829.

[45] MASTROPIETRO D G, MOYA J A. Design of Fe-based bulk metallic glasses for maximum amorphous diameter (D_{max}) using machine learning models [J]. Computational Materials Science, 2021, 188: 110230.

[46] MAJID A, AHSAN S B, TARIQ N U H. Modeling glass-forming ability of bulk metallic glasses using computational intelligent techniques [J]. Applied Soft Computing, 2015, 28: 569−578.

基于融合策略的块体金属玻璃形成能力预测

张 婷，龙志林，彭 黎

湘潭大学 土木工程学院，湘潭 411105

摘 要：提出一种融合策略来提高随机森林(RF)、k 近邻(KNN)、梯度提升决策树(GBDT)和极端梯度提升(XGBoost)模型预测块体金属玻璃(BMGs)形成能力(GFA)的准确性。该策略使用训练好的卷积神经网络(CNN)模型提取来特征向量，且合金的成分信息是唯一的输入变量，不需要通过实验获得其他物理和化学特性。此外，通过网格搜索方法和 k 折交叉验证对 RF、KNN、GBDT 和 XGBoost 模型的超参数进行了优化。结果表明，本文作者提出的 4 种融合模型 CNN−RF、CNN−KNN、CNN−GBDT 和 CNN−XGBoost 比上述 4 种机器学习模型(即 RF、KNN、GBDT 和 XGBoost 模型)预测精度更高，这表明训练好的 CNN 模型比人工特征提取更为高效。此外，与已报道的机器学习模型和 GFA 判据相比，本文作者提出的融合模型可以更精准地预测金属玻璃的形成能力。

关键词：块体金属玻璃；玻璃形成能力；机器学习；卷积神经网络；合金成分

(Edited by Wei-ping CHEN)